Journal of Scientific & Industrial Research
Vol. 81, April 2022, pp. 339-348

Adaptive Voltage and Current Control to Improve Stability and Restoration of Operation after the Occurrence of a Transient Fault in The Inverter-based Standalone Microgrid

Seyed Mohammad Shobeiry[1]*, Mohammad Taghi Ameli[1], Ali Oveysikian[2] and Ali Rahimi[3]

[1]Faculty of Electrical Engineering, Shahid Beheshti University, Tehran, Iran

[2]Faculty of Electrical Engineering, Islamic Azad University, North Tehran Branch, Tehran, Iran

[3]Faculty of Electrical Engineering, Semnan University, Semnan, Iran

Received 26 March 2021; revised 16 March 2022; accepted 16 March 2022

Small signal stability analysis and control strategies are well provided for conventional power systems. Still, in inverter-based microgrids, it is necessary to determine the model features and control specific oscillation modes. In this paper, inverter-based standalone microgrid performance modelling, including voltage and current control, has been developed. This model has inverter control loop details but does not provide switching performance. A simple adaptive controller controls the microgrid voltage and current, with only three parameters, including two negatively stable feedbacks and positive unstable feedback. Advantages of this controller over a Proportional Integral Derivative (PID) controller include proper adaptation to system changes, flexibility in setting up, and a robust deal with sudden changes in the system. Finally, by making drastic changes in the operation of a sample microgrid, such as loading and short circuit faults, we prove the effectiveness of the proposed adaptive control scheme in improving the stability and restoration of operation after the occurrence of a transient fault in the microgrid.

Keywords: Adaptive controller, Azadi controller, Distributed generation, Proportional integral derivative

Introduction

Recent innovations in Distributed Generation (DG) systems combined with outstanding advances in power electronics have led to the growing promotion of Microgrids (MGs). In traditional power systems, stability analysis and control schemes are well matured, and there are models with appropriate features for different issues and challenges. Reaching this point can be difficult for MGs due to the wide range of technologies.[1] Also, controlling systems with variable dynamics is one of the critical issues in power systems. Many researchers have used adaptive controllers; Calculating and adjusting the adaptive gains of controllers can be a daunting task. The complexity and timeliness of adaptive controller computations have also created many problems. The Azadi Controller is a fast and straightforward adaptive controller.[2] Ma *et al*.[3] provide a secondary voltage control for MGs using nonlinear multivariate adaptive control based on multiple models. This control scheme consists of two parts: 1- nonlinear adaptive controller based on neural network and a switching mechanism, 2- linear adaptive controller. Fattahi *et al*.[4] examine a droop control strategy based on adaptive fuzzy logic. This control is implemented by power electronic equipment to stabilize the bus AC voltage. Zhang *et al*.[5] investigate the coordinated problems of interconnected AC/DC MG power distribution. An appropriate control strategy has been developed to control the connected converter to achieve the proper power distribution between AC and DC MGs. The proposed approach consists of two parts: 1) dual-droop control method of the primary outer loop with secondary control. 2) Adaptive voltage control of the inner loop without a data-axis model. The main goal of the study by Holjevac *et al*.[6] is to determine the quantity of MG components' ability to provide flexibility. This flexibility defines the two operational principles of each MG: Standalone and connected to the grid with interacting and response to signals of the upstream system. Bidram *et al*.[7] have provided an adaptive secondary voltage control for MGs based on DGs inverter. In the proposed control structure, neural networks compensate for the uncertainty caused by the DG

*Author for Correspondence
E-mail: s_shobeiry@sbu.ac.ir

dynamics. Shi *et al*.[8] present a new DG control strategy using phasor measurement at a common connection point for MG islanding purposes. The proposed controller adapts the DG output to compensate for the power imbalance during transmission. Raghami *et al*.[9] propose a frequency control strategy for Inverter-based Standalone Microgrids (ISMGs) with two different load types: sensitive and variable based on the supply priority. The proposed method includes the primary and secondary control levels supported by a decommissioning plan. Primary control adjusts the DG's output power, while secondary control handles recovering the frequency after each load change.

Farzinfar *et al*.[10] have presented a combined protection-control scheme based on an Intelligent Electronic Device (IED) for MG. This scheme aims to ensure the continued stability of the ISMG. Roselyn *et al*.[11] propose an intelligent coordinated control strategy based on an adaptive neural-fuzzy inference system. The proposed plan improves voltage and frequency adjustment, reduces switching passes, and rapidly adapts demand changes. Afshari *et al*.[12] have proposed two new Distributed Fault Tolerance Control (DFTC) algorithms for voltage and frequency recovery in ISMGs. The proposed schemes against potential faults in sensors and actuators enable the fault-tolerant system. Elnady *et al*.[13] demonstrate the MG performance using a new adaptive PI controller-based control scheme. The core of the proposed control scheme is the adaptive PI controller. The PI controller parameters are adjustable, and no system model is required to work with this adaptive controller. To improve the dynamics and stability of DC bus voltage control, Zhang *et al*.[14] propose an adaptive sliding mode control method based on the large signal model. Siddique *et al*.[15] provide a modified adaptive PID controller for MGs. The objectives of this control include enhancing the voltage and current stability of the ISMG against various load dynamics. Ghazzali *et al*.[16] propose an adaptive power control strategy for autonomous MGs. This control is based on two methods: 1- Reference tracking to achieve an accurate division of active and reactive power, 2- Adaptive fixed-time control to ensure frequency and voltage regulation.

By examining the history of adaptive control of MGs, most studies are provided in the secondary control section. They have used complex methods for adaptive control, so in this paper, we offer a simple adaptive strategy to improve the primary control of MGs. This study aims to enhance the stability of ISMGs under different operating conditions, achieved by presenting and implementing a combined adaptive control plan with droop control.

This paper presents an MG's modelling and adaptive control of voltage and current inverters. Each inverter in DGs will have an external control function to share power with other DGs based on the droop. Internal inverter controls include new Adaptive Voltage Controllers (AVCs) and Adaptive Current Controllers (ACCs). A Common Reference Frame (CRF) uses a small-signal state-space model to implement the inverter model. The power controller adjusts the rotation frequency of this frame. The sample MG consists of three DGs with inverters implemented for validation in the MATLAB Simulink environment. The Innovation of this paper is the implementation of adaptive and straightforward control for voltage and current components and its combination with droop control in the primary control layer of DG sets that form an ISMG; due to this, the MG will have adaptive behaviour according to the conditions. It will offer a more stable and robust performance to deal with the severe changes in operation. After the occurrence of transient faults, it maintains its control and continues its regular and stable operation.

Materials and Methods

Azadi Adaptive Controller Model

Before introducing the adaptive controller model, we need to provide some concepts. We have three different responses for each typical control system, which has changed at different speeds. The reason for this behaviour change is the fault derivation parameter or $e'(t)$; the summary of its study is presented in Eq. (1):

$$\begin{cases} sluggish\ response\ e'(t) \ll 0 \\ rapid\ response\ e'(t) \gg 0 \end{cases} \quad ...(1)$$

Another crucial parameter to the system response is the fault rate or $e(t)$, In other words, the difference between the current performance of the system and the expected set point to be reached. Now we define a parameter that is very important in the controller performance. This parameter is obtained by dividing the error value by its derivative, and we specify it with V. The general form of this function is Eq. (2):

$$f(v) = \left|\frac{\sum_{i=0}^{n} \alpha_i v^i}{\sum_{i=0}^{n} \beta_i v^i}\right| . v = \left|\frac{e(t)}{\acute{e}(t)}\right| \quad ...(2)$$

The configuration of the Azadi adaptive controller is shown in Fig. 1. To adjust the system response, the function $f(v)$, which is conceptually a variable gain, is multiplied by the system error value. The standard controller used after multiplication ensures system stability; in fact, the Azadi controller is responsible for the main task of adaptive control.[2]

To clarify the function of this model, we consider the function $f(v)$ as Eq. (3):

$$f(v) = \frac{\alpha_0 - \alpha_1 v + \alpha_2 v^2}{1 + v + v^2} \quad ...(3)$$

This controller has only three parameters α_0, α_1, and α_2 for the setting. All these parameters are assumed to be positive. With this assumption, positive feedback by the coefficient α_1 may be generated and used for the system. A $f(v)$ is an adjustable gain; Therefore, to ensure the system stability, its final values, α_0 and α_2 must stabilize the system. In other words, the controller has one positive feedback term, which is limited to two negative feedback terms. Compared to a PID controller, this controller has the advantage of flexibility in adjusting and adapting the performance to cope with system changes. It is potent for compensating for system changes.[2] There is a function in nature with the same procedure as this controller. The concept of this function is the potential produced by nerve cells.[17,18]

MG Model in Standalone Operation

MG performance modes are divided into grid-connected or islanded from the grid. During operation in a grid-connected state, the power supply sources are controlled to supply the required power by the network; in other words, they are considered constant power sources that provide power without interruption. While in standalone mode, the power supply sources are controlled to provide the required power and preserve the frequency and voltage of the MG within the allowable limits. After disconnecting the MG from the main grid, the MG power sources maintain the voltage and frequency during power-sharing between loads. Throughout the islanded operation, the overloading of inverters should be avoided, and it should be ensured that the inverters provide load changes in an appropriately controlled manner.[1]

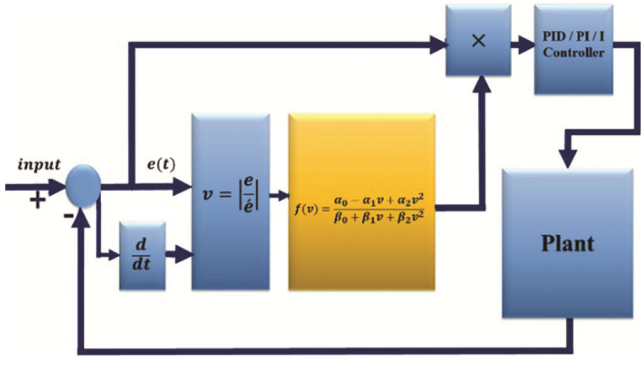

Fig. 1 — Implementation of Azadi Adaptive Controller configuration

As shown in Fig. 2, the modelling presented in this paper can be divided into three parts: an inverter, load, and network. The inverter model consists of the influential dynamics of the power-sharing controller, AVC and ACC, inductor, and output filter.

The DGs are connected via inverters; short response time and grid dynamics can affect system stability. First, the Reference Frame (RF) of one inverter is assumed to be the CRF. All other inverters are converted to this CRF using the conversion technique[19], also shown in Fig. 3. This concept is illustrated in Eq. (4) and (5).

In Fig. 3, the axis (D–Q) is expected to be the CRF that rotates with the frequency of ω_{com}; While the axes $(d-q)_i$ and $(d-q)_j$ are as the RF of the i and j inverters that rotate in ω_i and ω_j, respectively.

$$[f_{DQ}] = [T_i][f_{DQ}] \quad ...(4)$$

$$[T_i] = \begin{bmatrix} cos\,(\delta_i) & -sin\,(\delta_i) \\ sin\,(\delta_i) & cos\,(\delta_i) \end{bmatrix} \quad ...(5)$$

where, δ_i is the RF angle for inverter i concerning the CRF for all inverters.

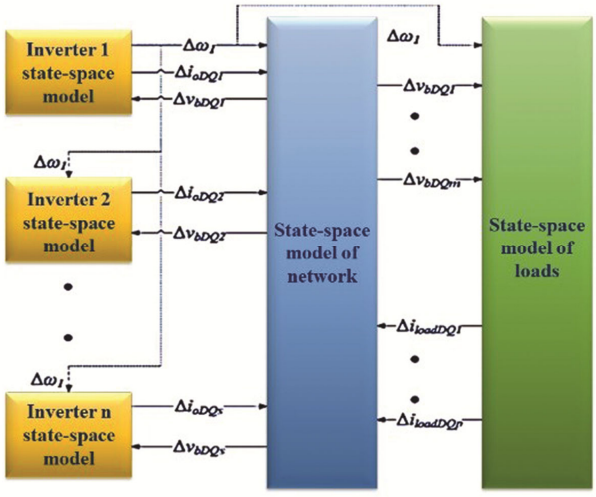

Fig. 2 — General scheme of an MG in state-space

DGs Inverter Configuration

The DG inverter is usually assumed to be the interface of DG in the MG. The configuration and internal details of an inverter are shown in Fig. 4. The inverter controller has three main parts. The first part has an external power control loop based on the droop rule that determines the value and frequency of the main component of the inverter output voltage. The second and third parts are AVCs and ACCs planned to throw away high-frequency disturbances. They also provide adequate damping for the LC output filter.[20]

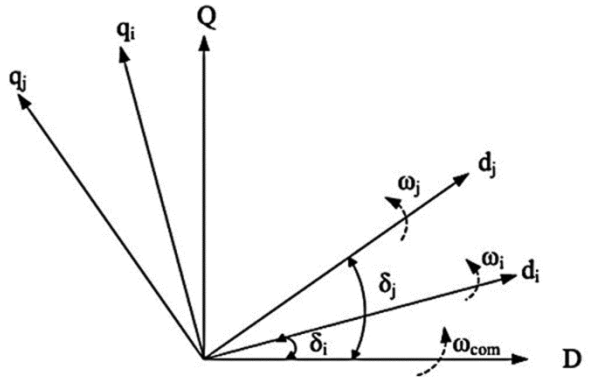

Fig. 3 — RF transformation

Therefore, following the droop control rule, power and frequency control is the power controller unit's responsibility. In this unit, the adaptive controller implementation is not desired because we want to maintain the benefits of droop control, and we leave this unit in the standard default mode.

On the other hand, the power controller output is the voltage controller input. Also, voltage and current controllers are the last blocks of signal control transmitted to the inverter, so they impose their control behaviour on the signal sent to the inverter; so these two blocks are good targets for implementing adaptive control because they offer adaptive behaviour for all the control components of the MG first layer to apply to the inverters. Normal voltage and current control blocks have a standard PI controller, which instead of the standard controller, an adaptive controller is implemented to improve control signals.

Power Controller

As shown in Fig. 5, the instantaneous active and reactive power terms, $\tilde{p}$ and, $\tilde{q}$ can be calculated with the output voltage and current through Eq. (6):

$$\tilde{p} = v_{od}i_{od} + v_{oq}i_{oq} \,.\, \tilde{q} = v_{od}i_{oq} - v_{oq}i_{od} \qquad \ldots (6)$$

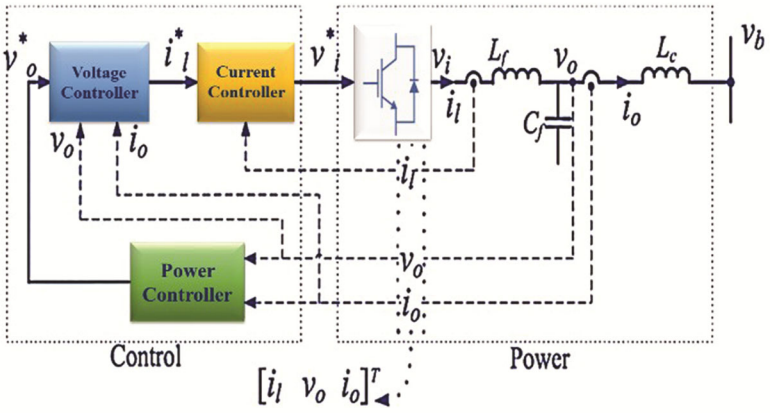

Fig. 4 — DG Inverter configuration

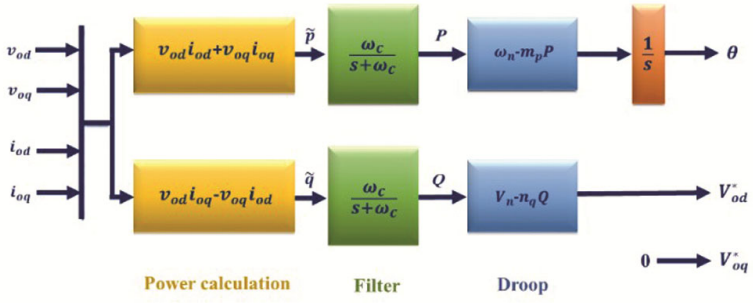

Fig. 5 — Power controller configuration

The instantaneous power terms are transmitted through low-pass filters to calculate the principal component's active and reactive power P and Q; the corresponding equations are presented in Eq. (7).

$$P = \frac{\omega_c}{s+\omega_c}\tilde{p} \,.\, Q = \frac{\omega_c}{s+\omega_c}\tilde{q} \qquad \ldots (7)$$

where, ω_n is the cut-off frequency. A forged droop in the frequency must be defined, presented in Eq. (8), to divide active power between the inverters. In the equations given below, α is the angle of the inverter RF seen from a rotating RF at ω_n and ω_n represents the nominal frequency adjustment point:

$$\omega = \omega_n - m_P P$$
$$\dot{\theta} = \omega \,.\, \theta = \omega_n t - \int m_P \, P dt$$
$$\alpha = -\int m_P \, P dt \,.\, \dot{\alpha} = -m_P P \qquad \ldots (8)$$

A voltage droop is introduced to share and circulate reactive power properly between the inverters in the MG, as shown in Eq. (9). Here v_n represents the nominal setting point of the output axis d of the output voltage.

$$v_{od}^* = v_n - n_q Q \,.\, v_{oq}^* = 0 \qquad \ldots (9)$$

Droop gains, i.e. m_p and n_q are calculated using Eq. (10) for the specified frequency range and voltage value.

$$mp = \frac{\omega_{max} - \omega_{min}}{p_{max}} \,.\, n_q = \frac{V_{od\,max} - V_{od\,min}}{Q_{max}} \qquad \ldots (10)$$

As mentioned earlier, to create a complete model in a CRF, one of the inverter's RF is optionally assumed to be a typical frame.

AVC Configuration

The voltage controller configuration is shown in Fig. 6. A simple adaptive controller (Azadi controller) controls the output voltage, while the model proposed by Pogaku *et al.*[1] uses a standard PI controller. Adjusting the voltage controller is more important and priority than the current controller. The power controller output is the voltage controller input directly, and the voltage controller output is the current controller input. Therefore, first, the coefficients were adjusted for the voltage adaptive control block, and finally, some additional modifications were applied by adjusting the coefficients of the ACC block. The main goal of implementing adaptive controllers is to improve control signals and provide signals according to the system behaviour. After implementing the AVC in the MG, the effect of a coefficient change on the adaptive controller response was examined. The following results were obtained: From left to right, respectively in the $f(v)$ numerator, the first coefficient handles eliminating the initial signal oscillation, the second coefficient compensates the overshoot, and finally, the third coefficient corrects the steady-state response. With numerous experiments, appropriate coefficients were extracted to obtain the best adaptive response is presented in Eq. (11). The function $f(v)$ used in the Azadi controller for adaptive voltage control is presented:

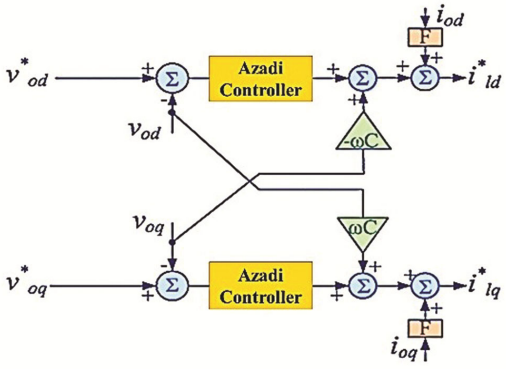

Fig. 6 — Voltage controller configuration

$$f(v) = \frac{0 \cdot 8 - 6v + 7 \cdot 5v^2}{1 + v + v^2} \qquad \ldots (11)$$

ACC Configuration

The configuration of the current control section is shown in Fig. 7. Output current control is achieved with a simple adaptive controller (Azadi controller), while a standard PI controller is used in the model proposed by Pogaku *et al.*[1] Adjustment coefficients of the ACC were adjusted for some additional modifications, and the significant adjustment of the adaptive behaviour is the AVC's responsibility. In Eq. (12), the function $f(v)$ used in the Azadi controller for current adaptive control is presented:

$$f(v) = \frac{4 - 6v + 7 \cdot 5v^2}{1 + v + v^2} \qquad \ldots (12)$$

Complete Single Inverter Model

The small-signal model of the output LC filter and the coupling inductor is checked, assuming that the inverter generates the required voltage. To integrate an inverter into an MG, output variables (currents) must be converted to a CRF. It ought tobe famous that the inverter, whose RF is considered a CRF, must provide its reference frequency for all subsets of the model.[1]

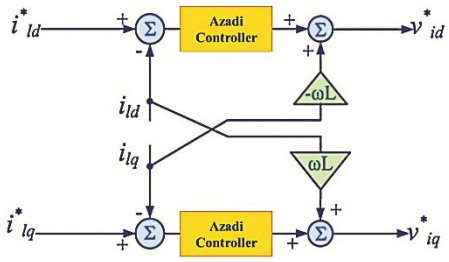

Fig. 7 — Current controller configuration

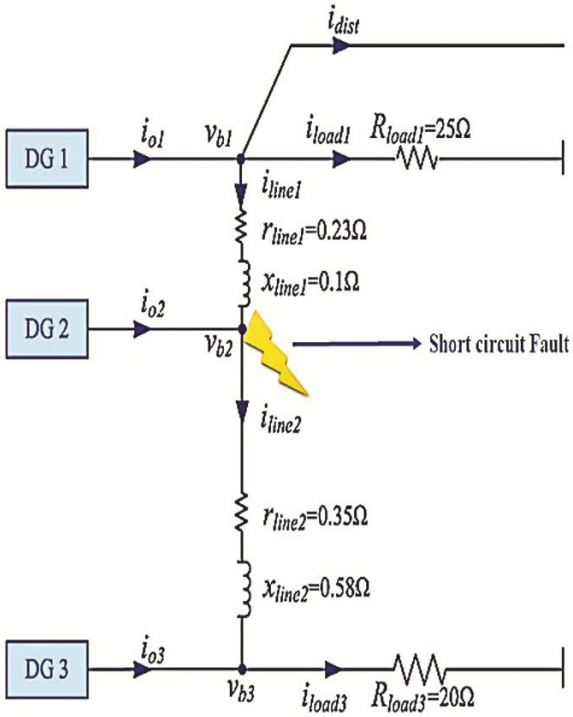

Fig. 8 — Test system

Experimental Validation

A sample MG with a voltage level of 220 V per phase and a frequency of 50 Hz for modelling validation is shown in Fig. 8. The implemented MG comprises three inverters with a nominal rate of 10 kVA and two resistive loads in buses 1 and 3. These inverters are controlled to properly share active and reactive power in the sample MG. The values of all specifications required for the test system are presented in Table 1. The grid in low voltage distribution systems is dominated by resistive mode. In this MG, the distances of DGs from each other are not equal.

In the sample MG, inverters have the same droop gain due to their equal size; in other words, they share power equally. There are many different energy sources in a natural environment, and droop gain may

Table 1 — Inverter specifications

Parameter	Value	Parameter	Value
	0.03 Ω		9.4e−5
	1.35 mH		1.3e−3
	0.1 Ω		4
	8 kHz		0.75
	50 μF		0.8
	31.41		6
	0.35 mH		7.5

be determined in terms of technical objectives and economic benefits and the tradeoff between them. The purpose of this paper is to investigate the system stability for the selected values of droop gains and the adaptive control of voltage and current under different operating conditions. The Azadi controller gains in the adaptive control of voltage and current were chosen to have good speed in response to each inverter and improved high-frequency disturbances. A low pass filter and significant droop gain are required to attenuate power-related high-frequency distortion terms and improve the DGs transient response.

The adaptive and combined control scheme presented in this paper has not been introduced so far; however, the standard mode1 in the voltage and current control section uses a simple PI controller. Our study's adaptive and hybrid control modes are in the experimental results section. During the changes in the operating conditions, our proposed Scheme provided good performance in terms of sustainability and adaptive control. To test the proposed scheme and its experimental validation, we considered two general and comprehensive MG models, including an MG with a standard PI controller in voltage and current controllers (common scheme) proposed by Pogaku *et al.*[1], and another MG with an Azadi controller instead of the standard PI controller in voltage and current controllers (suggested adaptive strategy) with a simulation time of 5 seconds. As shown in Fig. 8, two drastic changes were made in the MG. Entering a large load of 10 kW in the v_{b1} node near DG1 at 1 second, shown by i_{dist} As well as the occurrence of the worst type of short circuit fault, i.e. three-phases to the ground, at 2 to 2.05 seconds in the v_{b2} node, which can be the centre of the sample MG. These scenarios can demonstrate the proper performance of the proposed adaptive control for the sample MG stability. In a general view, the study flowchart is shown in Fig. 9.

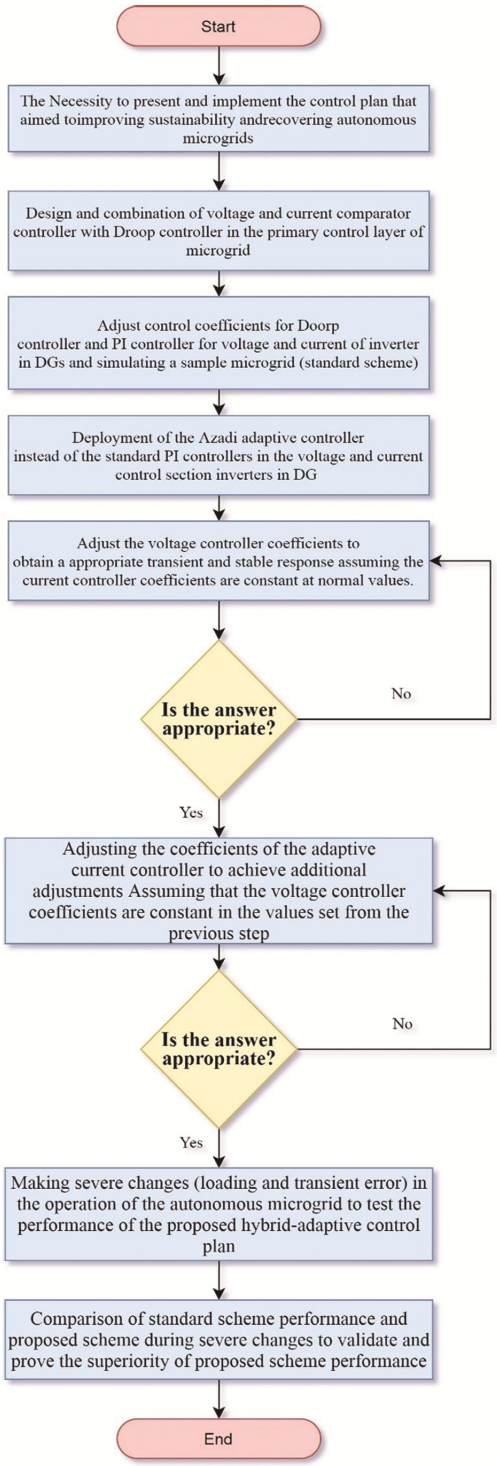

Fig. 9 — The study flowchart presented in this paper

Results and Discussion

During significant load changes, the DGs located near this change may be overloaded due to the inverter's limited loading capacity; So, we chose to enter a load of 10 kW near the relatively large DG1.

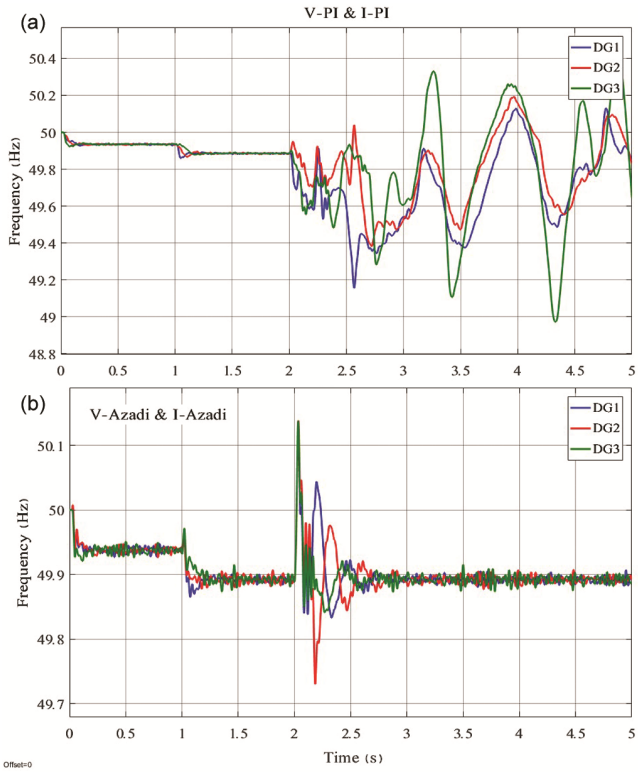

Fig. 10 — Frequency of all three DGs in a) standard control mode & b) adaptive control mode

First, we examine the standard scheme frequency (Fig. 10 a) and the proposed adaptive scheme frequency (Fig. 10 b). By comparing these two frequencies, it can be seen that with the entry of 10 kW load, the system with adaptive voltage and current control has a relatively faster response. In the case of short circuit faults, it is observed that the standard design has faced severe frequency fluctuations after the fault; While the adaptive system fixes these fluctuations in a maximum of 1 second and continues to control as before, even fluctuations amplitude is much lower in the adaptive state.

We now consider the active power, the active power of the standard mode (Fig. 11 a), and the active power of the adaptive mode (Fig. 11 b) are presented below. It is observed that in the standard mode, after the fault, there are severe fluctuations for the active power; while in adaptive mode, these fluctuations are controlled in a maximum of 1 second, the amplitude of the fluctuations is also much lower than the standard mode.

In the following, we examine the reactive power, the reactive power of the standard mode (Fig. 12 a), and the reactive power of the adaptive mode (Fig. 12 b). It is observed that in the standard mode,

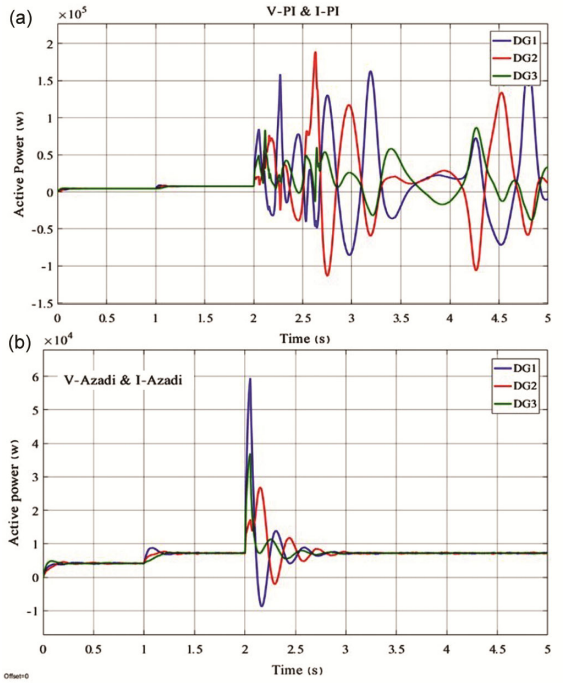

Fig. 11 — Active power of all three DGs in a) standard control mode & b) adaptive control mode

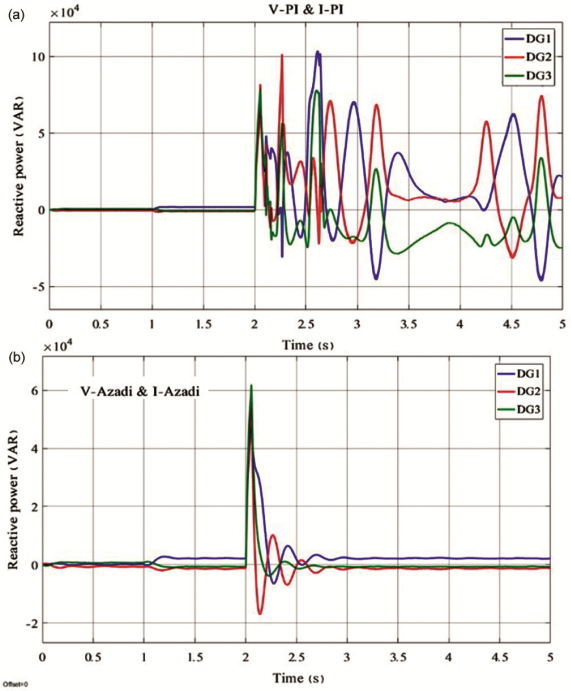

Fig. 12 — The reactive power of DGs in a) standard control mode & b) adaptive control mode

after the fault, there are severe fluctuations for the reactive power; While in adaptive mode, these fluctuations are controlled in a maximum of 1 second, the amplitude of the fluctuations is also much lower than the standard mode.

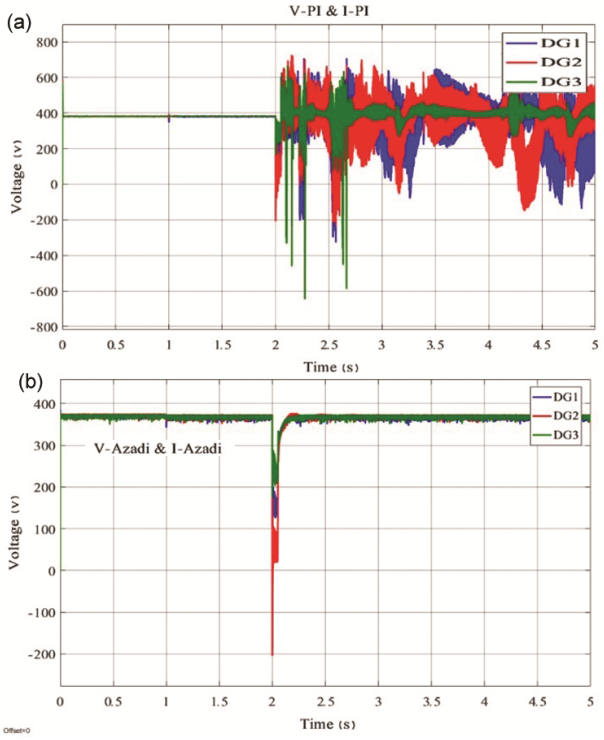

Fig. 13 — Component d of output voltage for all three DGs in a) standard control mode & b) adaptive control mode

Also, the output voltages d component, i.e. V_{od} for standard and adaptive mode are presented in Fig. 13 (a) and Fig. 13 (b), respectively. It is observed that severe high-frequency fluctuations occur after normal short circuit fault. In adaptive mode, the durability range of these fluctuations is only in the fault period (voltage control in 0.5 seconds), and the amplitude of the fluctuations is significantly reduced.

Finally, the output current d component, i.e. I_{od} for standard and adaptive modes is presented in Fig. 14 (a) and Fig. 14 (b), respectively. In the current waveform, severe high-frequency fluctuations occur in the standard mode after the fault occurs. These fluctuations are controlled less than 1 second after the fault period ends in adaptive mode.

To verify the results, we can refer to the proper performance of the Azadi adaptive controller in controlling different systems with variable dynamics, which[21] has well distinguished the appropriate interpretation of this controller compared to other controllers. Also, providing a standard mode and losing control after a transient fault and comparing it with the offered robust adaptive mode is an argument for accepting and using this adaptive controller instead of standard controllers such as a PI in current and voltage control of MGs.

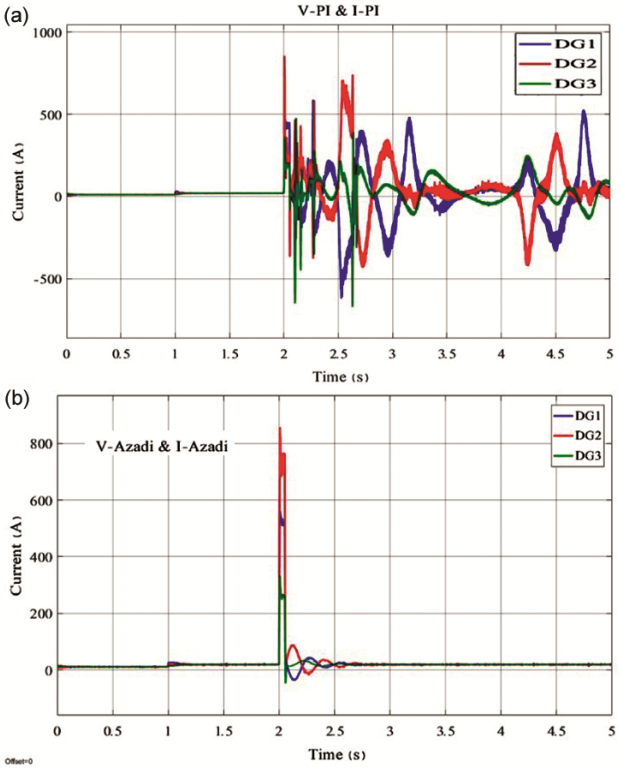

Fig. 14 — The output current d component for all three DGs in a) standard control mode & b) adaptive control mode

Conclusions

In this paper, the MG performance analysis is performed under the state-space model. All components were modelled separately and then combined to obtain the complete MG model. This study used a new control scheme based on the Droop and Azadi adaptive controllers to improve the ISMG's stability. It is worth noting that this paper's primary focus is on voltage and current adaptive control in the MG's primary control layer. Two MG voltage and current control schemes have been tested and compared to validate the proposed control function, including PI control, presented as a standard model of MG voltage and current control in previous research and Azadi control as a proposed model of MG voltage and current control in this research. The proposed model provides appropriate adaptive control under operating changes such as loading and the occurrence of three-phase short circuit fault to the ground. The MG is restored to a steady-state of operation after a transient fault. However, in the design based on PI control, the MG becomes permanently unstable after a transient fault occurs. These results reveal the advantage of using an Azadi adaptive control in ISMGs and highlight the need for further research and study on this controller in the future. For future research, the proposed control performance can be investigated in the presence of more DGs in the MG. Also, the effect of transient and dynamic faults can be studied using the proposed model.

References

1 Pogaku N, Prodanovic M & Green T C, Modeling, analysis and testing of autonomous operation of an inverter-based microgrid, *IEEE Trans Power Electron*, **22(2)** (2007) 613–625.

2 Azadi S, Introducing a simple adaptive controller (Azadi controller) based on positive feedbacks, in *Chin Control Decis Conf (CCDC)*, 2608–2613 May 2011.

3 Ma Z, Wang Z, Guo Y, Yuan Y & Chen H, Secondary Voltage Control of Microgrids Using Nonlinear Multiple Models Adaptive Control, *arXiv preprint arXiv*, **1810.09577** (2018).

4 Fattahi J, Schriemer H, Bacque B, Orr R, Hinzer K & Haysom J E, High stability adaptive microgrid control method using fuzzy logic, *Sustain Cities Soc*, **25** (2016) 57–64.

5 Zhang H, Zhou J, Sun Q, Guerrero J M & Ma D, Data-driven control for interlinked AC/DC microgrids via model-free adaptive control and dual-droop control, *IEEE Trans Smart Grid*, **8(2)** (2015) 557–571.

6 Holjevac N, Capuder T & Kuzle I, Adaptive control for evaluation of flexibility benefits in microgrid systems, *Energy*, **92** (2015) 487–504.

7 Bidram A, Davoudi A, Lewis F L & Ge S S, Distributed adaptive voltage control of inverter-based microgrids, *IEEE Trans Energy Convers*, **29(4)** (2014) 862–872.

8 Shi D, Sharma R & Ye Y, Adaptive control of distributed generation for microgrid islanding, in *IEEE PES ISGT Europe* 1–5 October 2013.

9 Raghami A, Ameli M T & Hamzeh M, Primary and secondary frequency control in an autonomous microgrid supported by a load-shedding strategy, in *4th Ann Int Power Electron, Drive Syst Technol Conf*, 282–287, February 2013.

10 Farzinfar M & Jazaeri M, Coordinated protection and control scheme for smooth transition from grid-connected to islanded mode of microgrids, *Iran J Sci Technol-Trans Electr Eng,* **44(2)** (2020) 911–926.

11 Roselyn J P, Ravi A, Devaraj D, Venkatesan R, Sadees M & Vijayakumar K, Intelligent coordinated control for improved voltage and frequency regulation with smooth switchover operation in LV microgrid, *Sustain Energy, Grids Netw*, **22** (2020) 100356.

12 Afshari A, Karrari M, Baghaee H R & Gharehpetian G B, Distributed fault-tolerant voltage/frequency synchronization in autonomous AC microgrids, *IEEE Trans Power Syst,* **35(5)** (2020) 3774–3789.

13 Elnady A & AlShabi M, Operation of parallel inverters in microgrid using new adaptive PI controllers based on least mean fourth technique, *Math Probl. Eng,* **19** (2019) 4854803.

14 Zhang D & Wang J, Adaptive Sliding-Mode Control in Bus Voltage for an Islanded DC Microgrid, *Math Probl. Eng*, **17** (2017) 8962086.

15 Siddique A B, Munsi M S, Sarker S K, Das S K & Islam M R, Voltage and current control augmentation of islanded microgrid using multifunction model reference modified adaptive PID controller, *Int J Electr Power Energy Syst*, **113** (2019) 492–501.

16 Ghazzali M, Haloua M & Giri F, Modeling and adaptive control and power sharing in islanded AC microgrids, *Int J Control Autom Syst*, **18.5** (2020) 1229–1241.

17 Kandel E R, Schwartz J H, Jessell T M, Siegelbaum S, Hudspeth A J & Mack S, *Principles of neural science* (McGraw-hill, New York) 2000, 1227–1246.

18 Guyton A C & Hall J E, *Textbook of Medical Physiology* (WB Saunders company, Philadelphia) 1986.

19 Uudrill J M, Dynamic stability calculations for an arbitrary number of interconnected synchronous machines, *Trans Power Appar Syst,* **3** (1968) 835–844.

20 Prodanovic M, *Power quality and control aspects of parallel connected inverters in distributed generation,* Ph D Thesis, Imperial College London, London, 2004.

21 Azadi S, Aghaei A & Hajimousa M A, Comparing Azadi Controller with Several Optimal Controllers, *Int J Basic Appl Sci (JBASR)*, **1(2)** (2013).